Synthesis, Characterization, and Biological Properties of Steroidal Ruthenium(II) and Iridium(III) Complexes Based on the Androst-16-en-3-ol Framework

Vanessa Koch,[†] Anna Meschkov,[†,‡] Wolfram Feuerstein,[§] Juliana Pfeifer,[‡] Olaf Fuhr,[∥] Martin Nieger,[⊥] Ute Schepers,[†,‡] and Stefan Bräse*[,†,#]

[†]Institute of Organic Chemistry (IOC), Karlsruhe Institute of Technology (KIT), Fritz Haber Weg 6, 76131 Karlsruhe, Germany

[‡]Institute of Functional Interfaces (IFG), Karlsruhe Institute of Technology (KIT), Hermann von Helmholtz Platz 1, 76344 Eggenstein Leopoldshafen, Germany

[§]Institute of Inorganic Chemistry, Division Molecular Chemistry, Karlsruhe Institute of Technology (KIT), Engesserstr. 15, 76131 Karlsruhe, Germany

[∥]Institute for Nanotechnology (INT) and Karlsruhe Nano Micro Facility (KNMF), Karlsruhe Institute of Technology (KIT), Hermann von Helmholtz Platz 1, 76344 Eggenstein Leopoldshafen, Germany

[⊥]Department of Chemistry, University of Helsinki, P.O. Box 55, 00014 Helsinki, Finland

[#]Institute of Toxicology and Genetics, Karlsruhe Institute of Technology (KIT), Hermann von Helmholtz Platz 1, D 76344 Eggenstein Leopoldshafen, Germany

ABSTRACT: A range of novel cyclometalated ruthenium(II) and iridium(III) complexes with a steroidal backbone based on androsterone were synthesized and characterized by NMR spectroscopy and X ray crystallography. Their cytotoxic properties in RT112 and RT112 cP (cisplatin resistant) cell lines as well as in MCF7 and somatic fibroblasts were compared with those of the corresponding nonsteroidal complexes and the noncyclometalated pyridyl complexes as well as with cisplatin as reference. All steroidal complexes were more active in RT112 cP cells than cisplatin, whereby the cyclometalated pyridinylphenyl complexes based on **5c** showed high cytotoxicity while maintaining low resistant factors of 0.33 and 0.50.

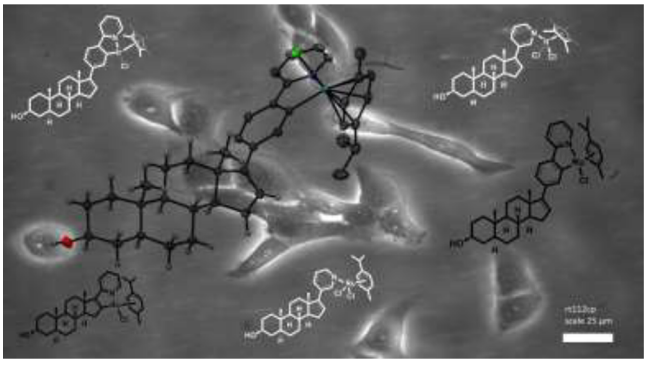

INTRODUCTION

Over the past 60 years, the interest in steroid bearing transition metal complexes has increased continuously.[1] In the late 1970s, the biological application of these complexes was discovered, enabling new perspectives for metal containing approaches, e.g., in the treatment of cancer.[1] Although platinum based anticancer complexes[2] such as cisplatin[3,4] or oxaliplatin[5,6] are worldwide recognized for the treatment of cancer, still some drawbacks remain. Diverse side effects as well as multifactorial drug resistance mechanisms, including, e.g., enhanced DNA repair, increased drug efflux, and detoxification, cause severe limitations in therapeutic use.[7,8] In order to circumvent intrinsic and acquired resistance and to reduce side effects, other transition metal based anticancer agents have been explored.[9] On the basis of ruthenium(III), KP1019[10] and NAMI A[11] (Figure 1) were developed, whereby both drugs already passed phase I of the clinical trials.[12−14] Ruthenium (III) probably serves as a pro drug and is reduced within the cell to the active ruthenium(II) complex. Noteworthy, ruthenium complexes of the type [Ru(η^6 arene)Cl_2(PTA)] (PTA = 1,3,5 triaza 7 phosphatricyclo[3.3.1.1]decane) also show promising anticancer properties and are therefore broadly investigated.[15−17] By connecting the metal center to a steroidal backbone as shown in complexes **1** and **2** (Figure 1), biological properties can be tuned. Since the steroidal framework enables the binding to steroid receptors, cell penetration can be improved. It has been also demonstrated that by the incorporation of a C 3 modified cholesterol ruthenium(III) complex **2** into a liposome bilayer, the ruthenium moiety was protected from degradation and the cellular uptake was favored. When integrated into a biomimetic membrane, the complex was found to be 6 fold times more active against the MCF 7 cell line (breast cancer) than the corresponding nonsteroidal complex.[18] Moreover, Jaouen et al.[19,20] and later Hannon et al.[21−24] could show that a sufficient

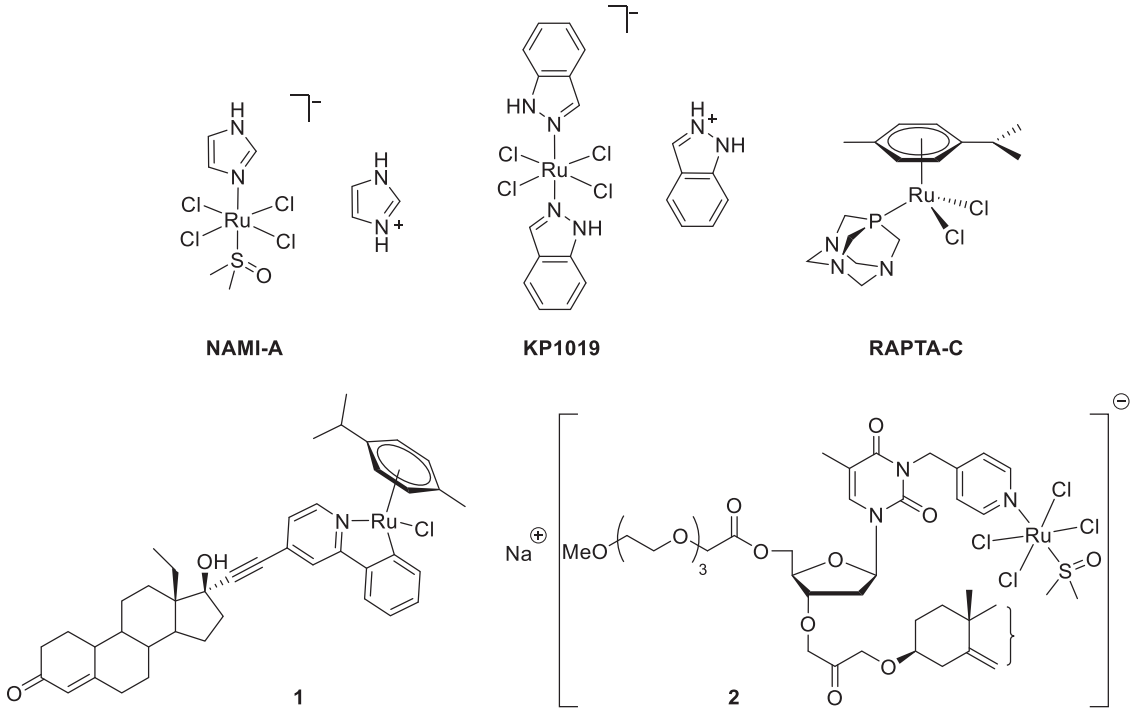

Figure 1. Currently investigated Ru(III) and Ru(II) anticancer drugs and ruthenium complexes based on an androgen (**1**) and a cholesterol (**2**) framework.

Scheme 1. Synthesis of the Steroidal Pyridine Containing Ligands 5 Starting from *epi* Androsterone (3) *via* a Two Step Procedure[31]

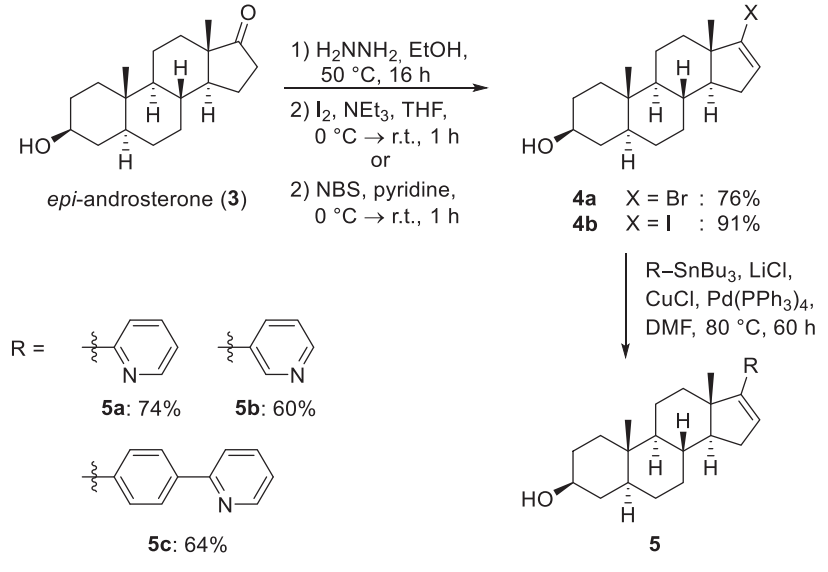

recognition of steroidal receptors is retained if the organo metallic site is attached at the end of a rigid spacer such as an ethynyl group at C 17 of an estradiol or testosterone derivative. In this context, Ruiz et al. found that the androgen containing ruthenium(II) complex **1** was 8 fold more active than cisplatin in T47D cell lines (breast cancer).[25,26] Lv et al. also reported an enhancement of the antiproliferative activity of an *N* heterocyclic carbene ruthenium complex in MCF 7 cells by conjugating a 17α ethynyl testosterone via a disulfide linkage.[27]

Compared to the number of studies on the anticancer activity of ruthenium complexes, only a few reports regarding the anticancer activity of iridium(III) complexes have been published.[25,28−30] Nevertheless, Sadler et al. showed that the biological activity of pentamethylcyclopentadienyl (Cp*)Ir (III) complexes was increased by the incorporation of phenyl substituents. This resulted in an enhanced cellular accumu lation due to the higher hydrophobicity of these complexes. Furthermore, the substitution of *N,N* ligands by *C,N* chelating ligands was shown to improve antiproliferative activity.

Motivated by these results, we envisioned to investigate the chemical, spectroscopic, and biological properties of novel ruthenium(II) and iridium(III) complexes based on *epi* androsterone with the metal center located closer to the steroidal backbone compared to previous examples.[25,26]

Scheme 2. Synthesis of Novel Cycloruthenated Ruthenium(II) Complexes 6, 7, and 8

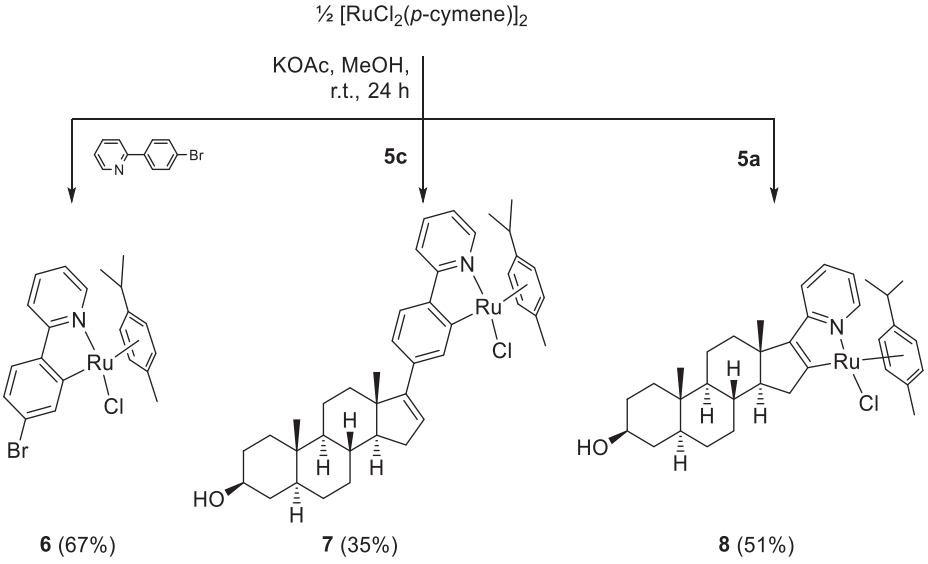

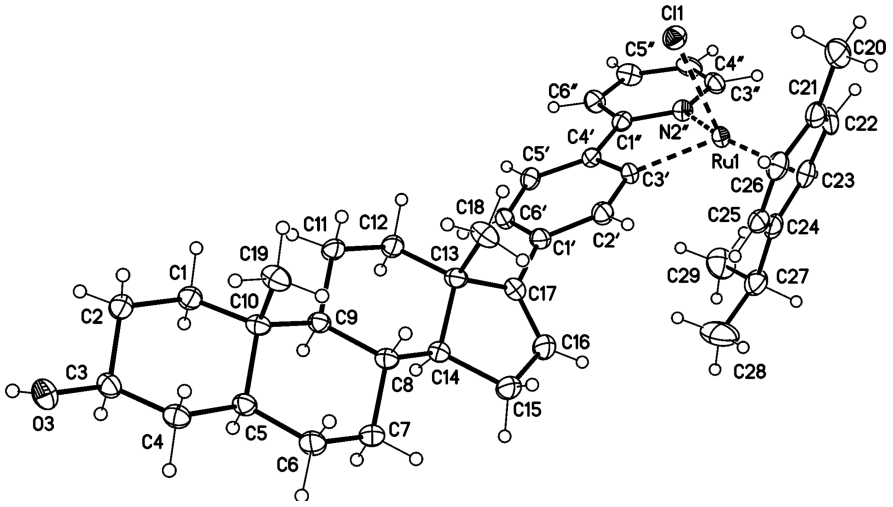

Figure 2. Molecular structure of the pyridylphenyl ruthenium(II) complex **7** (displacement parameters are drawn at 50% probability level). Characteristic bond lengths: Ru–N 2.097(3) Å; Ru–C 2.047(3) Å; Ru–Cl 2.4253(7) Å; Ru–C^{cymene} 2.154(3)–2.290(3) Å; Ru–$C^{cymene/centroid}$ 1.706(3) Å. Selected bond angles: N–Ru–C 77.72(12)°, N–Ru–Cl 86.98(3)°, Cl–Ru–C 85.76(9)°, N–Ru–cymene^{centroid} 132.3(1)°, Cl–Ru–cymene^{centroid} 126.6(1)°, C–Ru–cymene^{centroid} 130.3(1)°.

DESIGN AND SYNTHESIS OF THE NEW RUTHENIUM COMPLEXES

In order to bring the steroidal backbone in close proximity to the metal center, we aimed to modify C 17 of *epi* androsterone (**3**) in such a manner that the complexation of ruthenium(II) and the iridium(III) is feasible either by an *N* pyridine moiety or by κ^2 *N,C* cyclometalation. Therefore, different pyridine substituted androsterone derivatives (**5a**, **5b**) and a 4′ (2 pyridinyl)phenyl derivative (**5c**) were synthesized. As previously shown by our group, pyridine containing sub stituents are best introduced by the Stille cross coupling reaction.[31] Starting from *epi* androsterone (**3**), the desired ligands were easily accessible by a two step procedure (Scheme 1). Hence, *epi* androsterone (**3**) was treated with hydrazine to form the hydrazone giving either the alkenyl iodide **4a** by adding iodine in the presence of triethylamine or the alkenyl bromide **4b** by adding NBS with pyridine as a base. The following palladium catalyzed Stille cross coupling reac tion afforded the 2′ pyridinyl derivative **5a**, 3′ pyridinyl derivative **5b**, or 4 (pyridin 2′ yl)phenyl derivative **5c** in good yields ranging from 60–74%. By washing the obtained products **5** with *n* hexane, traces of remaining stannanes could be removed, which was crucial with regard to biological tests.

Since numerous procedures exist in the literature for the synthesis of cyclic ruthenium(II) complexes of 2 phenyl pyridines,[32−34] we tried analogous reaction conditions with 2 (4 bromophenyl)pyridine. With one equivalent of dimeric ruthenium precursor [Ru(η^6 *para* cymene)Cl_2]$_2$ and two equivalents of the ligand in the presence of four equivalents of KOAc in MeOH, the Ru(II) complex was formed after stirring at room temperature for 24 h. After flash column chromatography on silica gel, the ruthenium(II) complex **6** was isolated with 67% yield (Scheme 2). Applying the same reaction conditions, the synthesis of the phenylpyridinyl ruthenium(II) complex **7** and the pyridinyl ruthenium(II) complex **8** succeeded in moderate yields starting from their ligands **5c** or **5a** (Scheme 2).

Table 1. Experimental Proton and Carbon Resonances of the Diastereomers (*R* Ru) 8 and (*S* Ru) 8 and Their Experimental Differences of the Chemical Shifts $\Delta_\delta = \delta_S - \delta_R$ As Well As Their Differences $^{cal}\Delta_\delta = \delta_{(S)} - \delta_{(R)}$ Calculated on the TPSSh/def2 TZVPP Level of Theory Using bp86/def2 TZVPP Structures[a]

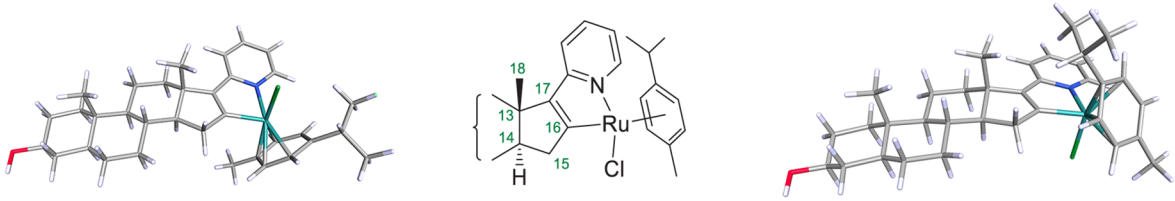

(*R*)-diastereomer **8** (*S*)-diastereomer

	(*R*)-diastereomer				(*S*)-diastereomer			
	^{13}C				^{1}H			
	δ_R [ppm]	$\Delta_{\delta(S\,R)}$[ppm]	δ_S [ppm]	$^{cal}\Delta_\delta$[ppm]	δ_R [ppm]	Δ_δ[ppm]	δ_S[ppm]	$^{cal}\Delta_\delta$[ppm]
16-C_q Ru	208.7	+1.0	209.7	+0.6				
17-C_q Pyr	150.4	+0.3	150.7	+0.2				
13-C_q	44.8	0.5	44.3	0.2				
18-CH_3	16.6	+0.8	17.4	+1.7	0.84	+0.09	0.93	+0.12
15α-CH_2	44.8	0.5	44.3	0.3	3.11	0.13	2.98	0.25
15β-CH_2					2.50	+0.34	2.84	+0.33
14-CH	58.5	0.2	58.3	+1.1	n.d.	n.d.	n.d.	0.01

[a]By comparing the calculated with experimental differences in chemical shifts, the diastereomers (*R* Ru) **8** and (*S* Ru) **8** were assigned. n.d. = not determined. See text for computational details.

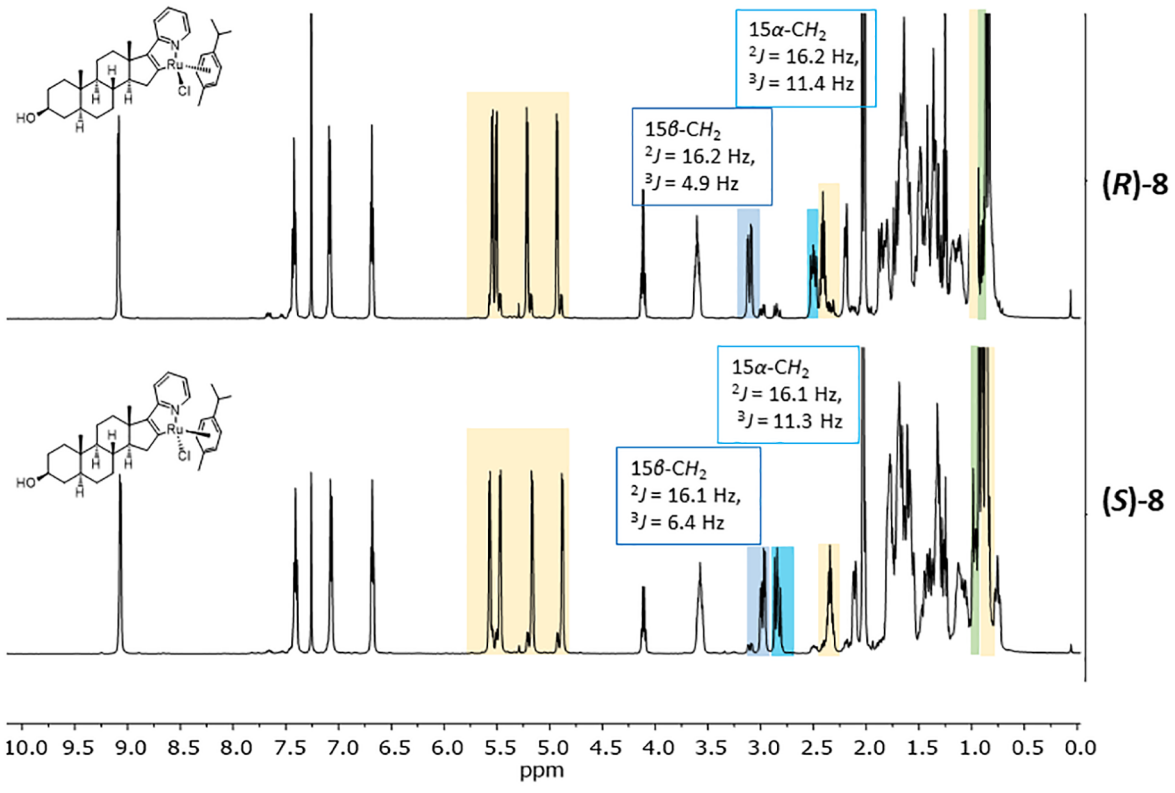

Figure 3. ^{1}H NMR spectra ($CDCl_3$, 500 MHz, r.t.) of the diastereomers (*R* Ru) **8** (top) and (*S* Ru) **8** (bottom). Significantly different shifts of the two diastereomers are highlighted (blue, 15 CH_2; yellow, cymene; green, 18 CH_3).

By recording ^{1}H and ^{13}C NMR, IR, and FAB mass spectra the complexes **6**, **7**, and **8** were successfully characterized. The Ru metal takes a pseudotetrahedral "piano stool" coordination geometry generating a new stereogenic center. Hence, most of the NMR resonances of the pyridinylphenyl ruthenium(II) complex **7** in d_1 chloroform were duplicated (see Supporting Information). DFT calculations on the BP86[35,36]/def2 TZVPP[37] level reveal the two diastereomers to differ only 5.6 kJ/mol in Gibbs free energy. Accordingly, both diastereomers were formed in comparable amounts as

evidenced by NMR signal intensities showing that no diastereomeric induction for cycloruthenation occurred. Furthermore, a single crystal suitable for X ray crystallography was obtained confirming the stated molecular structure for the *R* diastereomer as depicted in Figure 2. The coordination geometry of the Ru(II) center shows the expected pseudotetrahedral geometry. The N−Ru−C angle of 77.72(12)° is significantly smaller than the N−Ru−Cl (86.98(3)°) and the Cl−Ru−C (85.76(9)°) angles, which is in agreement with reported nonsteroidal cycloruthenated 2 phenylpyridinyl complexes.[38] In comparison with nonsteroidal complexes reported in the literature,[38,39] ruthenium(II) complexes **7** show similar bond angles and bond lengths, whereby Ru−X bond lengths (X = N, Cl, C) are slightly longer and bond angles Y−Ru−Z (Y≠ Z = N, Cl, C) slightly smaller. Unfortunately, we were not able to assign the crystal structure to one of the NMR signal sets, since the NMR chemical shifts of the diastereomers are too similar, as predicted by NMR shielding calculations (see Supporting Information).

Fortunately, in the case of the 2 pyridinyl ruthenium(II) complex **8**, the diastereomers could be separated by column chromatography on silica, whereby both diastereomers (*R* Ru) **8** and (*S* Ru) **8** were formed in equal amounts according to the integration of the crude ^{1}H NMR spectrum and could be isolated in comparable amounts. As for complex **7**, by optimizing the molecular structures of both diastereomers at the BP86[35,36]/def2 TZVPP[37] level of theory, we could show that none of the two diastereomers was noticeably thermodynamically favored standing in line with the nearly equimolar ratio of the isolated product. Both diastereomers showed nearly the same Gibbs free energies differing only by 3.2 kJ/mol in favor of the (*S*) diastereomer. In addition, we calculated ^{1}H and ^{13}C NMR shifts employing different density functionals using the optimized structures of both diastereomers to be compared with the experimental resonances. The TPSSh functional[40] turned out to yield the best accordance with the experimental NMR shift differences between (*R* Ru) **8** and (*S* Ru) **8** (see Supporting Information). This allowed for the assignment of the obtained NMR spectra to the two diastereomers (Table 1).

The corresponding ^{1}H NMR spectra and the relevant assignments are depicted in Figure 3. The stacked NMR spectra show no differences in chemical shifts for the proton resonances of the pyridinyl moiety. The aromatic and aliphatic proton resonances of the cymene ligand on the other hand, were clearly shifted similar to the three isopropyl resonances of (*S* Ru) **8** that appear at lower chemical shifts compared to the ones of (*R* Ru) **8**. Also, the resonances of the steroidal backbone close to the ruthenium center are affected by the different electronic environments of the two diastereomers. For example, in case of the diastereomer (*R* Ru) **8**, the methyl group and the chlorido substituent were located on the same side, resulting in a chemical shift of δ = 0.94 ppm, while the resonances of the diastereomer (*S* Ru) **8** are shifted upfield to δ = 0.84 ppm. Furthermore, the two diastereomeric 15 CH_2 resonances were influenced by the coordination to the pseudotetrahedral ruthenium center, whereby both signal sets were shifted downfield compared to those of the steroidal ligand **5b**. NOESY experiments and the evaluation of the coupling constants allowed the assignment of the more shielded signals to the 15β CH_2 protons, while the signals that arise more downfield belong to the 15α CH_2 protons, being in accordance with our calculations of the chemical shielding. It is noteworthy that for diastereomer (*S* Ru) **8**, the individual 15 CH_2 resonances were closer to each other than those for the diastereomer (*R* Ru) **8**, which was predicted by our chemical shielding calculations as well. This behavior is caused by the chlorido substituent: The nonbonding electrons lead to a shielding of spatially close protons by $n-\sigma^*$ interactions.[41] Hence, the β proton of diastereomer (*R* Ru) **8** is shifted to higher fields compared to its (*S* Ru) **8** counterpart. The same held true for the α proton of (*S* Ru) **8**, which is, however, less pronounced.

We were able to obtain a crystal structure of the (*R*) diastereomer of **8** (Figure 4) confirming the molecular

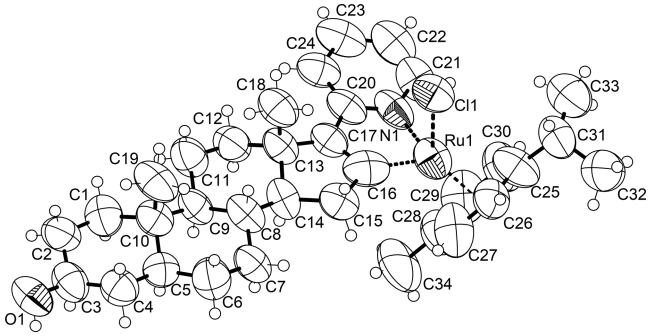

Figure 4. Molecular structure of the 2 pyridinyl ruthenium(II) complex (*R* Ru) **8** (displacement parameters are drawn at 50% probability level). Characteristic bond lengths: Ru−N 2.078(10) Å; Ru−C 1.931 Å; Ru−Cl 2.415(3) Å; Ru−cymene 2.130(16)−2.341(14) Å; Ru−cymene/centroid 1.729 Å. Selected bond angles: N−Ru−C 76.3(4)°, N−Ru−Cl 85.2(2)°, Cl−Ru−C 86.4(3)°, N−Ru−cymene^{centroid} 132.33°, Cl−Ru−cymene^{centroid} 126.60°, C−Ru−cymene^{centroid} 130.34°.

structure and the correct assignments of the diastereomers based on the calculated chemical shifts. In contrast to the phenylpyridinyl ruthenium(II) complex **6** and its steroidal counterpart **7**, the Ru−C bond of (*R* Ru) **8** is significantly shorter (1.931 Å vs 2.062 Å of **6**[39]/2.047 Å of **7**). This is an indication for the inferior electron donating ability of the cyclopentenido moiety of the steroidal D ring compared to phenyl. To the best of our knowledge, the herein presented ruthenium complex **8** is the first example of a cyclopentenido pyridinyl ruthenium(II) complex.[42,43]

Furthermore, comparable iridium(III) complexes were synthesized by applying similar reaction conditions and $[IrCp^*Cl_2]_2$ as a metal precursor. The three cyclometalated Ir(III) complexes **9**, **10**, and **11** (Scheme 3) were synthesized in overall good yields, whereby the diastereomers of **10** and **11** were formed in equal amounts giving two sets of signals in the ^{1}H and ^{13}C NMR spectra. Unfortunately, a separation of the diastereomers **11** via column chromatography was not successful.

For comparison with the cycloruthenated complexes **7** and **8** as well as for the analogous iridium(III) complexes **10** and **11**, (17 (3′ pyridinyl)androsten)dichloride ruthenium(II) complex **12** and the corresponding iridium(III) complex **13** were synthesized by stirring two equivalents of the ligand **5b** and one equivalent of the dimeric metal precursor in dichloromethane (Scheme 4). After precipitation with *n* hexane, the metal complexes **12** and **13** were obtained in good yields.

We were able to obtain crystal structures suitable for crystal structure analysis for both 3 pyridyl complexes **12** and **13**

Scheme 3. Synthesis of Novel Cyclometalated Iridium(III) Complexes 9, 10, and 11

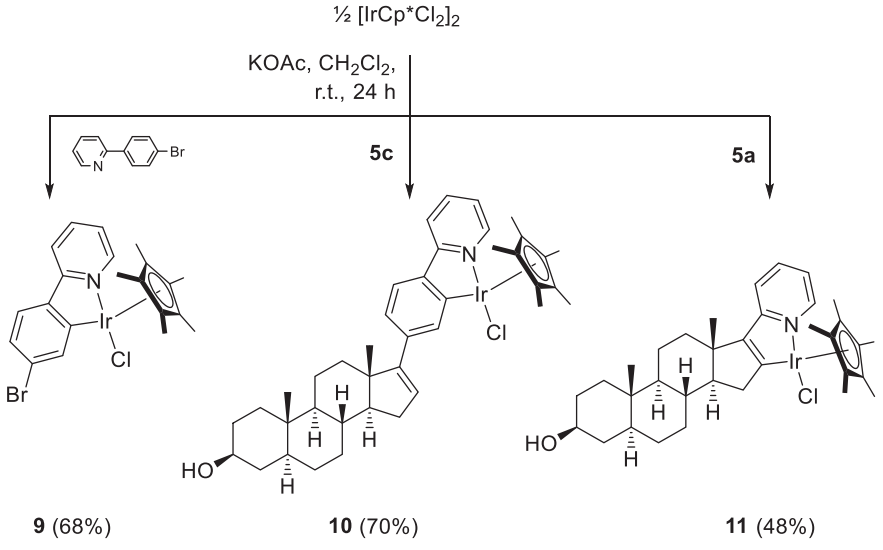

Scheme 4. Synthesis of the (17 (3′ Pyridinyl)androstenido)dichloride Ruthenium(II) Complex 12 and the Corresponding Iridium(III) Complex 13

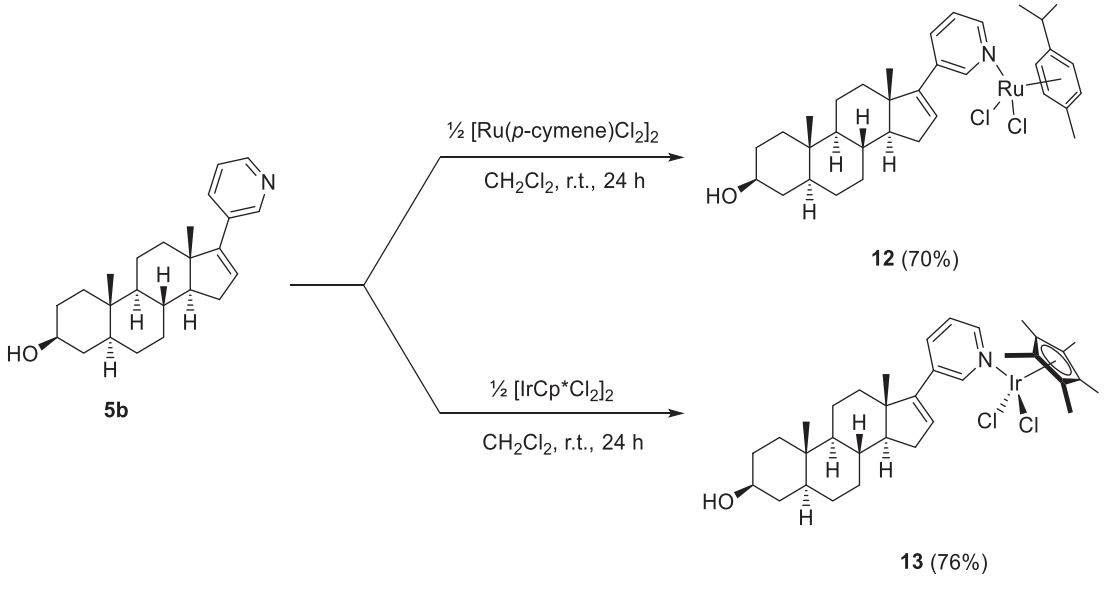

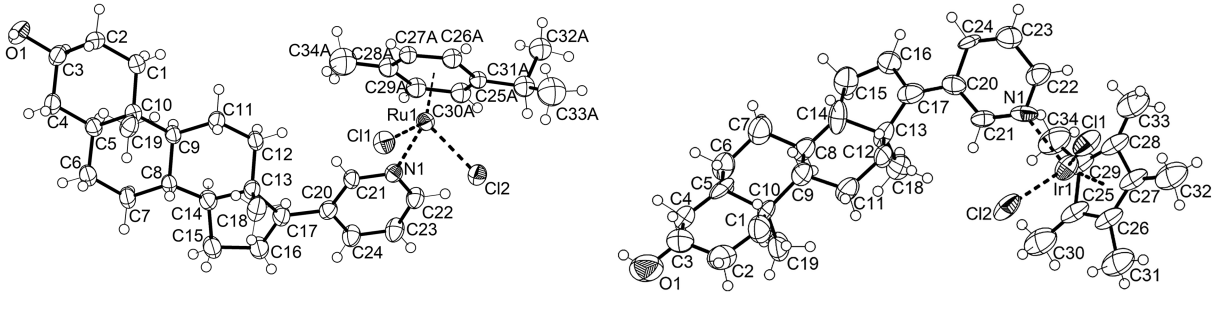

Figure 5. Molecular structure of the 3 pyridyl ruthenium(II) complex **12** (left) and the 3 pyridyl iridium(III) **13** (right). The cymene ligand of ruthenium(II) complex **12** is disordered. Selected bond lengths for **12**/**13**: Ru−N 2.125(3) Å; Ru−C^{cymene} 2.159(10)−2.231(10) Å; Ru−$Cl^{(1)}$ 2.419 Å; Ru−$Cl^{(2)}$ 2.404 Å/Ir−$Cl^{(1)}$ 2.395(5) Å; Ir−$Cl^{(2)}$ 2.408(6) Å; Ir−N 2.090(5) Å; Ir−C^{Cp*} 2.11(2)−2.26(2) Å; Ir−$C^{Cp*/centroid}$ 1.788 Å. Selected bond angles for **12**/**13**: $Cl^{(1)}$−Ir−$Cl^{(2)}$ 89.2(2)°; N−Ir−$Cl^{(1)}$ 85.9(5)°; N−Ir−$Cl^{(2)}$ 85.6(5)°; N−Ir−$C^{Cp*/centroid}$ 125.7(2)°; $Cl^{(1)}$−Ir−$C^{Cp*/centroid}$ 127.4(8)°; $Cl^{(2)}$−Ir−$C^{Cp*/centroid}$ 128.9(5)°/$Cl^{(1)}$−Ru−$Cl^{(2)}$ 87.4(7)°; N−Ru−$Cl^{(1)}$ 85.2(1)°; N−Ir−$Cl^{(2)}$ 84.9(0)°.

(Figure 5), confirming their molecular structure and the pseudotetrahedral coordination geometry around the metal. Interestingly, in the solid state, the nitrogen atom of the pyridyl moiety points toward the 18 methyl group and the metal atoms were located on the upper side of the steroidal framework. It is noteworthy that the ruthenium(II) complex **12** shows almost no distortion (6.81°) in contrast to the free ligand **5b** (see Supporting Information for the crystal structure) and the iridium(III) complex **13** whose pyridine units are twisted to the D ring plane with a torsion of 32.9(3)° or 29.1(8)°.

BIOLOGICAL ACTIVITY AND CYTOTOXICITY STUDIES

To evaluate the cytotoxicity of the compounds, an *in vitro* MTT assay was performed (Table 2). The MTT (3 (4,5 dimethylthiazol 2 yl) 2,5 diphenyltetrazolium bromide) reagent can be reduced to blue purple formazan by the mitochondrial enzymes of living cells. The amount of resulting formazan can be determined photometrically and correlates directly with the cell viability, since this reaction can only take place in metabolically active cells. The cytotoxicity was tested in different tumor and somatic cells including bladder cancer cells, which show resistance to cisplatin and breast cancer cells (MCF7), which usually show hormone dependency. In order to test a potential application in cisplatin resistant cells, the human bladder carcinoma cell line RT112 and its cisplatin resistant counterpart RT112 cP were cultivated with varying concentrations (0.5−50 μM) of the ruthenium(II) (**6**, **7**, **8**, and **12**) and iridium(III) complexes (**9**, **10**, **11**, and **13**), and the cell viability was monitored after 72 h of incubation. In addition, the cytotoxicity of the free ligands ((4 bromophenyl)pyridine, **5a**−**5c**) and cisplatin was evaluated for comparison. There are some reports on the expression of various steroid receptors in bladder cancer cells,[44,45] assuming that steroidal ligands could have an effect. All complexes demonstrated higher cytotoxicity against RT112 cP cells compared to cisplatin (IC_{50} values 1−11 μM and >50 μM, respectively). The cytotoxicity of the complexes **8** (both (*S*) and (*R*) diastereomers), **11**, **12**, and **13** was in the same order of magnitude as that of the corresponding free steroidal ligands (**5a** and **5b**), with IC_{50} values in the range between 2.5 and 7.5 μM for both cell lines. However, the steroidal ligand **5c** demonstrated high biocompatibility (IC_{50} > 50 μM for both cell lines), whereas the corresponding Ru(II) (**7**) and Ir(III) (**10**) complexes showed promising antiproliferative effects in both cell lines. This indicates that the cisplatin resistance was successfully overcome with IC_{50} values of 1 μM for RT112 cP cells and very low resistance factors of 0.33 and 0.5, respectively. Although the nonsteroidal complexes **6** and **9** were also more toxic (IC_{50} 5−8 μM) compared to the free nonsteroidal (4-bromophenyl)pyridine ligand (IC_{50} > 50 μM), the steroidal complexes **7** and **10** were significantly more effective with considerably lower IC_{50} values and resistance factors. For the MCF 7 cells, all the steroid complexes demonstrated a high cytotoxic activity with IC_{50} values in the range of 2.5−8.5 μM, significantly more effective as cisplatin with an IC_{50} value of 22.5 μM. The Ru(II) complex **7** was slightly more active in comparison to the corresponding ligand **5c** (IC_{50} values 2.5 and 6.6 μM, respectively). Moreover, the cytotoxic activity of the majority of the compounds was lower for NHDF compared to the cancer cell lines, with especially high IC_{50} values for the complexes **12** and **13** (>50 μM), suggesting a therapeutic window with a selectivity for cancer cells.

Table 2. IC_{50} Values and Resistance Factors (RF, $IC_{50(resistant)}/IC_{50(sensitive)}$) of the Ru(II) and Ir(III) Complexes, Free Ligands, and Cisplatin (μM)

entry	compound	RT112	RT112 cP (RF)	MCF-7	NHDF
1	(4-bromophenyl) pyridine	>50.0	>50.0	>50.0	>50.0
2	Ru(II) complex **6**	5.0	5.0 (1.00)	5.5	5.5
3	Ir(III) complex **9**	7.5	8.0 (1.07)	40.0	35.0
4	ligand **5a**	2.5	2.0 (0.80)	3.3	8.0
5	Ru(II) complex **8** (*S*)/(*R*) 1:1	3.5	6.5 (1.86)	6.3	9.1
6	(*S*-Ru) complex **8**	2.5	5.5 (2.20)	6.0	10.5
7	(*R*-Ru) complex **8**	3.9	6.0 (1.54)	5.5	7.0
8	Ir(III) complex **11**	4.5	2.5 (0.56)	5.7	6.9
9	ligand **5b**	7.5	7.0 (0.93)	9.0	>50.0
10	Ru(II) complex **12**	9.0	7.5 (0.83)	7.0	>50.0
11	Ir(III) complex **13**	9.0	11.0 (1.22)	8.5	>50.0
12	ligand **5c**	>50.0	>50.0	6.6	>50.0
13	Ru(II) complex **7**	3.0	1.0 (0.33)	2.5	5.5
14	Ir(III) complex **10**	2.0	1.0 (0.50)	8.5	17.5
15	cisplatin	3.5	>50.0	22.5	>50.0

CONCLUSION

In conclusion, a set of Ru(II) and Ir(III) complexes with different *N* containing ligands based on a steroidal backbone was synthesized and characterized by NMR spectroscopy and X ray crystallography. All evaluated complexes showed high cytotoxicity in the tested cancer cell lines and were more active in RT112 cP and MCF 7 cells than cisplatin. Remarkable is the very low resistant factor of the complexes in the range between 0.33 and 1.22, indicating successful overcoming of the cisplatin resistance. Especially promising results were obtained for the complexes **7** and **10** with the steroidal ligand **5c**, since the advantageous high biocompatibility of **5c** (IC_{50} > 50 μM) was combined with a pronounced antiproliferative effect of the complexes **7** (IC_{50} 3 μM for RT112 and 1 μM for RT112 cP) and **10** (IC_{50}2 μM for RT112 and 1 μM for RT112 cP) with resistant factors 0.33 and 0.5, respectively. In breast cancer cells, which show a proliferation dependency on hormone expression, all complexes showed an effective cytotoxicity including the complex **7** (IC_{50} = 2.5 μM). This antiproliferative activity was significantly higher than for the well established ruthenium complexes RAPTA T and NAMI A, with IC_{50} values >200 μM and 800 μM (both MCF 7), reported by Nazarov et al.[46] and Pluim et al.,[47] respectively. The cytotoxic effect of the compounds was also higher than that of the mentioned cholesterol ruthenium(III) complex incorporated into a liposome bilayer, demonstrated by Simeone et al. (IC_{50} of about 70 μM),[18] and was in the range of the testosterone−ruthenium conjugate described by Lv et al. (IC_{50} of about 4.5 μM).[27] Furthermore, the complexes showed a promising selectivity for the cancer cells, exhibiting lower cytotoxicity against normal fibroblasts compared to the tested cancer cell lines.

EXPERIMENTAL SECTION

Instrumental Measurements. ATR IR spectra were performed on Bruker alpha p and a FT IR IFS 88 spectrometer. ^{1}H and ^{13}C

NMR spectra were recorded on different types of Bruker Avance 400, Bruker Avance III HD, or Bruker Avance 600 spectrometer with residual proton signals of the deuterated solvent as the internal standard. EI and FAB mass spectra (positive mode) were measured on a Finnigan MAT95. Further information is given in the Supporting Information.

General Procedure for Metallacyclization Reactions with Ruthenium(II) and Iridium(III). Under an argon atmosphere, the ligand (2.00 equiv), $[RuCl_2(p\ cymene)]_2$ (1.00 equiv) or $[IrCp^*Cl_2]_2$ (1.00 equiv), and KOAc (4.00 equiv) were dissolved in dry MeOH or CH_2Cl_2 and stirred at room temperature for 24 h. The suspension was concentrated, and the residue was purified by flash column chromatography on silica gel to obtain the cyclometalated complexes as yellow to orange solids. The reactions based on a steroidal ligand were performed on a 30−120 μmol scale.

Crystal Structure Determinations. The single crystal X ray diffraction study of **5b**[31] and **7** was carried out on a Bruker D8 Venture diffractometer with a Photon100 detector at 123(2) K using Cu−Kα radiation (λ = 1.54178 Å). Direct Methods (SHELXS 97)[48] was used for structure solution, and refinement was carried out using SHELXL 2014 (full matrix least squares on F^2).[49] Hydrogen atoms were localized by difference electron density determination and refined using a riding model (H(O) free). Semiempirical absorption corrections were applied. The absolute configuration was determined by refinement of Parsons' x parameter.[50] The single crystal X ray diffraction study of (*R* Ru) **8**, **12**, and **13** was performed on a *Stoe StadiVari* diffractometer using Ga Kα radiation (λ = 1.34143 Å) generated by an Metaljet X ray source. The crystals were kept at 180.15 K during data collection. Using Olex2,[51] the structures were solved with the ShelXS[48] structure solution program using Direct Methods and refined with the ShelXL[49] refinement package using Least Squares minimization. Non hydrogen atoms were refined with anisotropic displacement parameters; hydrogen atoms were modeled on idealized positions.

CCDC 1521243 (**5b**), 1859054 (**7**), 1944097 ((*R* Ru) **8**), 1944098 (**12**), and 1944099 (**13**) contain the supplementary crystallographic data for this paper. These data can be obtained free of charge from the Cambridge Crystallographic Data Centre via www.ccdc.cam.ac.uk/data request/cif.

Computational Details. Structure optimizations were done on the BP86[35,36]/def2 TZVPP[37] level of theory using the TURBOMOLE 7.1 program package.[52] Solvent effects of chloroform were taken into account with the COSMO solvation model.[53] The RI approximation was used throughout.[54] Stationary points were verified to be minimum energy structures by numerically calculating the molecular Hessian and analyzing the so obtained vibrational frequencies. The numerical frequencies were used to calculate thermodynamic properties at 298.15 K and 1 bar in harmonic and ideal gas approximations. NMR chemical shifts were calculated on the basis of Gauge Including Atomic Orbitals (GIAO).[55]

Cell Culture. RT112 (human bladder carcinoma cell line), RT112 cP (cisplatin resistant), NHDF (normal human dermal fibroblasts), and MCF 7 (breast cancer cell line) were cultured in RPMI (Roswell Park Memorial Istitute) medium (Gibco, for RT112 and RT112 cP) or DMEM (Dulbecco's modified eagle medium, Gibco, for NHDF and MCF 7) supplemented with 10% fetal bovine serum (FBS, Gibco) and 1% penicillin/streptavidin (Gibco) at 37 °C, 5% CO_2, and a humid atmosphere. For all *in vitro* experiments, cells were trypsinized (0.05% trypsin EDTA, Gibco) and seeded in 96 well plates (toxicity assay) at the required densities. Incubation was performed under the culture conditions as described above.

Cytotoxicity Assay. RT112 (human bladder carcinoma cell line), RT112 cP (cisplatin resistant), NHDF (normal human dermal fibroblasts), and MCF 7 (breast cancer cell line) were seeded in the 96 well plates at a density of 1×10^4 cells/well in RPMI (RT112 and RT112 cP) medium or DMEM (NHDF and MCF 7) supplemented with 10% FCS and 1% penicillin/streptomycin. After 24 h of incubation at 37 °C and 5% CO_2, the medium was removed and the cells were treated with various concentrations of the compounds in the corresponding culture medium and incubated for 72 h at 37 °C and 5% CO_2. The stock solutions of the compounds were prepared in DMSO and the end concentration of the solvent in the test dilutions was held under 0.5%. Since the cytotoxic activity of cisplatin was shown to be affected by DMSO,[56] a stable 5 mM stock solution of cisplatin in $DPBS^{-/-}$ (Gibco) was prepared. As a negative control, the cell culture medium was exchanged without addition of the compounds. Thereafter, 15 μL of the MTT reagent (Promega) was given in each well. For the positive control, Triton X 100 (1%) was added in some wells before treating them with the MTT reagent. After 3 h of incubation, the cells were lysed using the Stop Solution (Promega) to release the blue purple formazan. The cell viability was determined by measuring the absorbance of the resulting formazan at 595 nm using a multiwell plate reader (SpectraMax ID3, Molecular Devices, USA) and calculated in relation to the negative control.

■ ASSOCIATED CONTENT

● Supporting Information

The Supporting Information is available free of charge on the ACS Publications website at DOI: 10.1021/acs.inorgchem.9b02402.

Additional spectroscopic data, experimental and computational details, and characterization data (PDF)

Accession Codes

CCDC 1859054 and 1944097−1944099 contain the supplementary crystallographic data for this paper. These data can be obtained free of charge via www.ccdc.cam.ac.uk/data request/cif, or by emailing data request@ccdc.cam.ac.uk, or by contacting The Cambridge Crystallographic Data Centre, 12 Union Road, Cambridge CB2 1EZ, UK; fax: +44 1223 336033.

■ AUTHOR INFORMATION

Corresponding Author

*E mail: braese@kit.edu.

ORCID

Vanessa Koch: 0000 0002 2115 3124

Stefan Bräse: 0000 0003 4845 3191

Author Contributions

The manuscript was written through contributions of all authors. All authors have given approval to the final version of the manuscript.

Notes

The authors declare no competing financial interest.

■ ACKNOWLEDGMENTS

We acknowledge the DFG Core Facility MOLECULE ARCHIVE (grant numbers: BR1750/40 1, JU2909/5 1) for the management and provision of the compounds for screening. V.K. gratefully acknowledges the Studienstiftung des Deutschen Volkes and W.F., the Carl Zeiss Stiftung for financial support. The work was supported by the Deutsche Forschungsgemeinschaft (DFG), within the Research Training Group 2039 (A.M., U.S. S.B.) and the Helmholtz Program Biointerfaces in Technology and Medicine (BIFTM; U.S., A.M., S.B.). We thank Prof. Dr. Frank Breher for supporting this cooperation, Dr. Beate Köberle for providing cell lines, and Magdalena Winklhofer for assistance in *in vitro* experiments.

■ REFERENCES

(1) Le Bideau, F.; Dagorne, S. Synthesis of Transition Metal Steroid Derivatives. *Chem. Rev.* **2013**, *113* (10), 7793−7850.

(2) Wilson, J. J.; Lippard, S. J. Synthetic Methods for the Preparation of Platinum Anticancer Complexes. *Chem. Rev.* **2014**, *114* (8), 4470−4495.

(3) Rosenberg, B.; Van Camp, L.; Krigas, T. Inhibition of Cell Division in Escherichia coli by Electrolysis Products from a Platinum Electrode. *Nature* **1965**, *205*, 698.
(4) Rosenberg, B. V. C.; Grimley, L.; Eugene, B.; Thomson, A. J. The Inhibition of Growth or Cell Division in Escherichia coli by Different Ionic Species of Platinum(IV) Complexes. *J. Biol. Chem.* **1967**, *242*, 1347−1352.
(5) Faivre, S.; Chan, D.; Salinas, R.; Woynarowska, B.; Woynarowski, J. M. DNA strand breaks and apoptosis induced by oxaliplatin in cancer cells. *Biochem. Pharmacol.* **2003**, *66* (2), 225−237.
(6) Raymond, E.; Chaney, S. G.; Taamma, A.; Cvitkovic, E. Oxaliplatin: A review of preclinical and clinical studies. *Ann. Oncol.* **1998**, *9* (10), 1053−1071.
(7) Florea, A. M.; Büsselberg, D. Cisplatin as an anti tumor drug: cellular mechanisms of activity, drug resistance and induced side effects. *Cancers* **2011**, *3* (1), 1351−1371.
(8) Galluzzi, L.; Senovilla, L.; Vitale, I.; Michels, J.; Martins, I.; Kepp, O.; Castedo, M.; Kroemer, G. Molecular mechanisms of cisplatin resistance. *Oncogene* **2012**, *31* (15), 1869−1883.
(9) Ang, W. H.; Casini, A.; Sava, G.; Dyson, P. J. Organometallic ruthenium based antitumor compounds with novel modes of action. *J. Organomet. Chem.* **2011**, *696* (5), 989−998.
(10) Lentz, F.; Drescher, A.; Lindauer, A.; Henke, M.; Hilger, R. A.; Hartinger, C. G.; Scheulen, M. E.; Dittrich, C.; Keppler, B. K.; Jaehde, U. Pharmacokinetics of a novel anticancer ruthenium complex (KP1019, FFC14A) in a phase I dose escalation study. *Anti Cancer Drugs* **2009**, *20* (2), 97−103.
(11) Alessio, E. Thirty Years of the Drug Candidate NAMI A and the Myths in the Field of Ruthenium Anticancer Compounds: A Personal Perspective. *Eur. J. Inorg. Chem.* **2017**, *2017* (12), 1549−1560.
(12) Rademaker Lakhai, J. M.; van den Bongard, D.; Pluim, D.; Beijnen, J. H.; Schellens, J. H. M. A Phase I and Pharmacological Study with Imidazolium *trans* DMSO imidazole tetrachlororuthenate, a Novel Ruthenium Anticancer Agent. *Clin. Cancer Res.* **2004**, *10* (11), 3717−3727.
(13) Hartinger, C. G.; Jakupec, M. A.; Zorbas Seifried, S.; Groessl, M.; Egger, A.; Berger, W.; Zorbas, H.; Dyson, P. J.; Keppler, B. K. KP1019, A New Redox Active Anticancer Agent Preclinical Development and Results of a Clinical Phase I Study in Tumor Patients. *Chem. Biodiversity* **2008**, *5* (10), 2140−2155.
(14) Leijen, S.; Burgers, S. A.; Baas, P.; Pluim, D.; Tibben, M.; van Werkhoven, E.; Alessio, E.; Sava, G.; Beijnen, J. H.; Schellens, J. H. M. Phase I/II study with ruthenium compound NAMI A and gemcitabine in patients with non small cell lung cancer after first line therapy. *Invest. New Drugs* **2015**, *33* (1), 201−214.
(15) Babak, M. V.; Meier, S. M.; Huber, K. V. M.; Reynisson, J.; Legin, A. A.; Jakupec, M. A.; Roller, A.; Stukalov, A.; Gridling, M.; Bennett, K. L.; Colinge, J.; Berger, W.; Dyson, P. J.; Superti Furga, G.; Keppler, B. K.; Hartinger, C. G. Target profiling of an antimetastatic RAPTA agent by chemical proteomics: relevance to the mode of action. *Chem. Sci.* **2015**, *6* (4), 2449−2456.
(16) Gasser, G.; Ott, I.; Metzler Nolte, N. Organometallic Anticancer Compounds. *J. Med. Chem.* **2011**, *54* (1), 3−25.
(17) Hartinger, C. G.; Metzler Nolte, N.; Dyson, P. J. Challenges and Opportunities in the Development of Organometallic Anticancer Drugs. *Organometallics* **2012**, *31* (16), 5677−5685.
(18) Simeone, L.; Mangiapia, G.; Vitiello, G.; Irace, C.; Colonna, A.; Ortona, O.; Montesarchio, D.; Paduano, L. Cholesterol Based Nucleolipid Ruthenium Complex Stabilized by Lipid Aggregates for Antineoplastic Therapy. *Bioconjugate Chem.* **2012**, *23* (4), 758−770.
(19) Top, S.; El Hafa, H.; Vessières, A.; Huché, M.; Vaissermann, J.; Jaouen, G. Novel Estradiol Derivatives Labeled with Ru, W, and Co Complexes. Influence on Hormone Receptor Affinity of Several Organometallic Groups at the 17α Position. *Chem. Eur. J.* **2002**, *8* (22), 5241−5249.
(20) Vessières, A.; Top, S.; Vaillant, C.; Osella, D.; Mornon, J. P.; Jaouen, G. Estradiols Modified by Metal Carbonyl Clusters as Suicide Substrates for the Study of Receptor Proteins: Application to the Estradiol Receptor. *Angew. Chem., Int. Ed. Engl.* **1992**, *31* (6), 753−755.
(21) Huxley, M.; Sanchez Cano, C.; Browning, M. J.; Navarro Ranninger, C.; Quiroga, A. G.; Rodger, A.; Hannon, M. J. An androgenic steroid delivery vector that imparts activity to a non conventional platinum(II) metallo drug. *Dalton Trans.* **2010**, *39* (47), 11353−11364.
(22) Sanchez Cano, C.; Huxley, M.; Ducani, C.; Hamad, A. E.; Browning, M. J.; Navarro Ranninger, C.; Quiroga, A. G.; Rodger, A.; Hannon, M. J. Conjugation of testosterone modifies the interaction of mono functional cationic platinum(II) complexes with DNA, causing significant alterations to the DNA helix. *Dalton Trans.* **2010**, *39* (47), 11365−11374.
(23) Sanchez Cano, C.; Hannon, M. J. Cytotoxicity, cellular localisation and biomolecular interaction of non covalent metallo intercalators with appended sex hormone steroid vectors. *Dalton Trans.* **2009**, No. 48, 10765−10773.
(24) Jackson, A.; Davis, J.; Pither, R. J.; Rodger, A.; Hannon, M. J. Estrogen Derived Steroidal Metal Complexes: Agents for Cellular Delivery of Metal Centers to Estrogen Receptor Positive Cells. *Inorg. Chem.* **2001**, *40* (16), 3964−3973.
(25) Ruiz, J.; Rodriguez, V.; Cutillas, N.; Samper, K. G.; Capdevila, M.; Palacios, O.; Espinosa, A. Novel C, N chelate rhodium(III) and iridium(III) antitumor complexes incorporating a lipophilic steroidal conjugate and their interaction with DNA. *Dalton Trans.* **2012**, *41* (41), 12847−12856.
(26) Ruiz, J.; Rodríguez, V.; Cutillas, N.; Espinosa, A.; Hannon, M. J. A Potent Ruthenium(II) Antitumor Complex Bearing a Lipophilic Levonorgestrel Group. *Inorg. Chem.* **2011**, *50* (18), 9164−9171.
(27) Lv, G.; Qiu, L.; Li, K.; Liu, Q.; Li, X.; Peng, Y.; Wang, S.; Lin, J. Enhancement of therapeutic effect in breast cancer with a steroid conjugated ruthenium complex. *New J. Chem.* **2019**, *43* (8), 3419−3427.
(28) Millett, A. J.; Habtemariam, A.; Romero Canelón, I.; Clarkson, G. J.; Sadler, P. J. Contrasting Anticancer Activity of Half Sandwich Iridium(III) Complexes Bearing Functionally Diverse 2 Phenyl pyridine Ligands. *Organometallics* **2015**, *34* (11), 2683−2694.
(29) Liu, Z.; Habtemariam, A.; Pizarro, A. M.; Fletcher, S. A.; Kisova, A.; Vrana, O.; Salassa, L.; Bruijnincx, P. C. A.; Clarkson, G. J.; Brabec, V.; Sadler, P. J. Organometallic Half Sandwich Iridium Anticancer Complexes. *J. Med. Chem.* **2011**, *54* (8), 3011−3026.
(30) Liu, Z.; Habtemariam, A.; Pizarro, A. M.; Clarkson, G. J.; Sadler, P. J. Organometallic Iridium(III) Cyclopentadienyl Anticancer Complexes Containing *C,N* Chelating Ligands. *Organometallics* **2011**, *30* (17), 4702−4710.
(31) Koch, V.; Nieger, M.; Bräse, S. Stille and Suzuki Cross Coupling Reactions as Versatile Tools for Modifications at C 17 of Steroidal Skeletons A Comprehensive Study. *Adv. Synth. Catal.* **2017**, *359* (5), 832−840.
(32) Li, B.; Darcel, C.; Roisnel, T.; Dixneuf, P. H. Cycloruthenation of aryl imines and *N* heteroaryl benzenes via C H bond activation with Ru(II) and acetate partners. *J. Organomet. Chem.* **2015**, *793*, 200−209.
(33) Özdemir, I.; Demir, S.; Çetinkaya, B.; Gourlaouen, C.; Maseras, F.; Bruneau, C.; Dixneuf, P. H. Direct Arylation of Arene C H Bonds by Cooperative Action of NHCarbene Ruthenium(II) Catalyst and Carbonate via Proton Abstraction Mechanism. *J. Am. Chem. Soc.* **2008**, *130* (4), 1156−1157.
(34) Ferrer Flegeau, E.; Bruneau, C.; Dixneuf, P. H.; Jutand, A. Autocatalysis for C H Bond Activation by Ruthenium(II) Complexes in Catalytic Arylation of Functional Arenes. *J. Am. Chem. Soc.* **2011**, *133* (26), 10161−10170.
(35) Becke, A. D. Density functional exchange energy approxima tion with correct asymptotic behavior. *Phys. Rev. A: At., Mol., Opt. Phys.* **1988**, *38* (6), 3098−3100.
(36) Perdew, J. P. Density functional approximation for the correlation energy of the inhomogeneous electron gas. *Phys. Rev. B: Condens. Matter Mater. Phys.* **1986**, *33* (12), 8822−8824.

(37) Weigend, F.; Ahlrichs, R. Balanced basis sets of split valence, triple zeta valence and quadruple zeta valence quality for H to Rn: Design and assessment of accuracy. *Phys. Chem. Chem. Phys.* **2005**, *7* (18), 3297−3305.
(38) Nam, J. P.; Park, S. C.; Kim, T. H.; Jang, J. Y.; Choi, C.; Jang, M. K.; Nah, J. W. Encapsulation of paclitaxel into lauric acid O carboxymethyl chitosan transferrin micelles for hydrophobic drug delivery and site specific targeted delivery. *Int. J. Pharm.* **2013**, *457* (1), 124−35.
(39) Djukic, J. P.; Berger, A.; Duquenne, M.; Pfeffer, M.; de Cian, A.; Kyritsakas Gruber, N.; Vachon, J.; Lacour, J. Syntheses of Nonracemic Ortho Mercurated and Ortho Ruthenated Complexes of 2 [Tricarbonyl(η^6 phenyl)chromium]pyridine. *Organometallics* **2004**, *23* (24), 5757−5767.
(40) Tao, J.; Perdew, J. P.; Staroverov, V. N.; Scuseria, G. E. Climbing the Density Functional Ladder: Nonempirical Meta Generalized Gradient Approximation Designed for Molecules and Solids. *Phys. Rev. Lett.* **2003**, *91* (14), 146401.
(41) Lambert, J. B.; Mazzola, E. P. *Nuclear Magnetic Resonance Spectroscopy: An Introduction to Principles, Applications, and Exper imental Methods*; Pearson Education, 2004.
(42) Coalter, J. N.; Streib, W. E.; Caulton, K. G. Reactivity of $[RuHCl(P^iPr_3)_2]_2$ with Functionalized Vinyl Substrates. The H2 Ligand as a Sensitive Probe of Electronic Structure. *Inorg. Chem.* **2000**, *39* (17), 3749−3756.
(43) Zhang, L.; Dang, L.; Wen, T. B.; Sung, H. H. Y.; Williams, I. D.; Lin, Z.; Jia, G. Cyclometalation of 2 Vinylpyridine with $MCl_2(PPh_3)_3$ and $MHCl(PPh_3)_3$ (M = Ru, Os). *Organometallics* **2007**, *26* (11), 2849−2860.
(44) Shen, S. S.; Smith, C. L.; Hsieh, J. T.; Yu, J.; Kim, I. Y.; Jian, W.; Sonpavde, G.; Ayala, G. E.; Younes, M.; Lerner, S. P. Expression of estrogen receptors α and β in bladder cancer cell lines and human bladder tumor tissue. *Cancer* **2006**, *106* (12), 2610−2616.
(45) Nakashiro, K. i.; Hayashi, Y.; Kita, A.; Tamatani, T.; Chlenski, A.; Usuda, N.; Hattori, K.; Reddy, J. K.; Oyasu, R. Role of peroxisome proliferator activated receptor γ and its ligands in non neoplastic and neoplastic human urothelial cells. *Am. J. Pathol.* **2001**, *159* (2), 591−597.
(46) Nazarov, A. A.; Meier, S. M.; Zava, O.; Nosova, Y. N.; Milaeva, E. R.; Hartinger, C. G.; Dyson, P. J. Protein ruthenation and DNA alkylation: chlorambucil functionalized RAPTA complexes and their anticancer activity. *Dalton Trans.* **2015**, *44* (8), 3614−3623.
(47) Pluim, D.; van Waardenburg, R. C. A. M.; Beijnen, J. H.; Schellens, J. H. M. Cytotoxicity of the organic ruthenium anticancer drug Nami A is correlated with DNA binding in four different human tumor cell lines. *Cancer Chemother. Pharmacol.* **2004**, *54* (1), 71−78.
(48) Sheldrick, G. A short history of SHELX. *Acta Crystallogr., Sect. A: Found. Crystallogr.* **2008**, *64* (1), 112−122.
(49) Sheldrick, G. Crystal structure refinement with SHELXL. *Acta Crystallogr., Sect. C: Struct. Chem.* **2015**, *71* (1), 3−8.
(50) Parsons, S.; Flack, H. D.; Wagner, T. Use of intensity quotients and differences in absolute structure refinement. *Acta Crystallogr., Sect. B: Struct. Sci., Cryst. Eng. Mater.* **2013**, *69* (3), 249−259.
(51) Dolomanov, O. V.; Bourhis, L. J.; Gildea, R. J.; Howard, J. A. K.; Puschmann, H. OLEX2: a complete structure solution, refinement and analysis program. *J. Appl. Crystallogr.* **2009**, *42* (2), 339−341.
(52) *TURBOMOLE V7.1*; TURBOMOLE GmbH, 2016. Available from http://www.turbomole.com.
(53) Klamt, A.; Schuurmann, G. COSMO: a new approach to dielectric screening in solvents with explicit expressions for the screening energy and its gradient. *J. Chem. Soc., Perkin Trans. 2* **1993**, No. 5, 799−805.
(54) Sierka, M.; Hogekamp, A.; Ahlrichs, R. Fast evaluation of the Coulomb potential for electron densities using multipole accelerated resolution of identity approximation. *J. Chem. Phys.* **2003**, *118* (20), 9136−9148.
(55) Schreckenbach, G.; Ziegler, T. Calculation of NMR Shielding Tensors Using Gauge Including Atomic Orbitals and Modern Density Functional Theory. *J. Phys. Chem.* **1995**, *99* (2), 606−611.
(56) Hall, M. D.; Telma, K. A.; Chang, K. E.; Lee, T. D.; Madigan, J. P.; Lloyd, J. R.; Goldlust, I. S.; Hoeschele, J. D.; Gottesman, M. M. Say no to DMSO: dimethylsulfoxide inactivates cisplatin, carboplatin, and other platinum complexes. *Cancer Res.* **2014**, *74* (14), 3913−3922.